MECHANICAL ANALOGS OF COEXISTENT PHASES

E. Chater and J. W. Hutchinson

1. INTRODUCTION

Certain mechanical systems display transitions between two nominally uniform solution states which have certain features in common with true phase transitions. Three such examples will be discussed here. In order, they are the bulging of a long cylindrical balloon, neck propagation along bars of certain polymeric materials, and buckle propagation along externally pressurized pipes. Most of the results presented here were taken from two earlier papers by the authors and a colleague [1, 2].

2. STEADY-STATE INFLATION OF A CYLINDRICAL PARTY BALLOON

Imagine a long party balloon with a long uniform cylindrical section in its mid-region. The properties of most balloon rubbers are such that the pressure-volume relation of a cylindrical slice undergoing a purely cylindrical deformation has the qualitative features shown in Fig. 1. The balloon is treated as a membrane with thickness small compared to radius. A purely cylindrical deformation is defined as a deformation in which the slice is imagined to undergo a uniform expansion of its radius and a uniform axial elongation such that the circumferential and axial stresses,

PHASE TRANSFORMATIONS AND MATERIAL INSTABILITIES IN SOLIDS

ISBN 0-12-309770-3

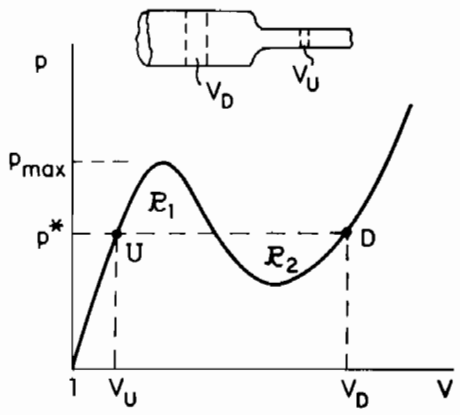

Fig. 1 p(V) for purely cylindrical deformation of a cylindrical segment of unit initial volume. Quasi-static, steady-state propagation requires $\mathcal{R}_1 = \mathcal{R}_2$. (Figure taken from [1].)

respectively, are given by $\sigma_\theta = pR/t$ and $\sigma_x = pR/(2t)$ where R is the current radius, t is the current thickness and p is the internal pressure. The slice considered in Fig. 1 is taken to have a unit volume in the undeformed state. For definiteness it will be assumed that the balloon is inflated under isothermal conditions, and the purely cylindrical deformation in Fig. 1 should also be regarded as isothermal.

The relation of pressure to change of volume of the entire balloon during the inflation process is depicted in Fig. 2. As air is forced into the balloon, a localized bulge forms somewhere along the length of the balloon, usually at one of the ends. The pressure peaks with the initial bulge formation. With continued inflation the pressure settles down to a constant value, p* in Fig. 2, and during this part of the process the transition front between the bulged and unbulged regions simply translates down the length of the balloon with essentially no change in radii of the regions on either side of the transition. This is the portion of the inflation process we will refer to as steady-state propagation. If the balloon is inflated slowly, as is

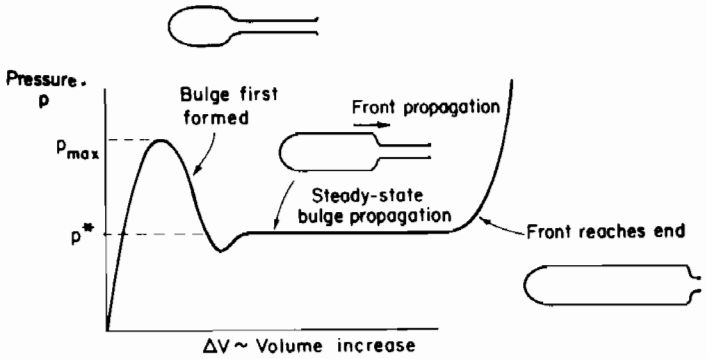

Fig. 2 Inflation of a cylindrical party balloon. (Figure taken from [1].)

assumed to be the case, inertial effects are negligible and the propagation is quasi-static. An example of a partially inflated party balloon is shown in Fig. 3. When the transition front has engulfed the whole balloon the pressure rises and the mid-region again undergoes essentially purely cylindrical deformations.

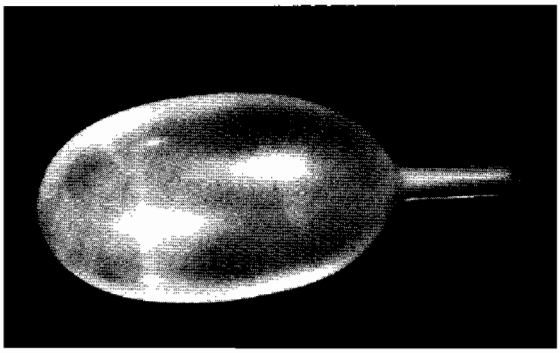

Fig. 3 Party balloon showing transition between bulged and unbulged sections. (Figure taken from [1].)

The equation for the steady-state, quasi-static propagation pressure p^* is obtained by a very simple energy balance argument. Namely, the work done by p^* must equal the change of strain energy stored in the balloon in a unit advance of the transition front. Model the mid-region of the balloon by an infinitely long balloon with uniform properties. Let V_D and V_U denote the volumes of cylindrical sections, each with unit undeformed volume, associated with purely cylindrical deformation states U and D far ahead and far behind, respectively, the transition. These states are each associated with p^* as indicated in Fig. 1. Under steady-state conditions in which the front engulfs a new section with unit undeformed volume, the work done by p^* is exactly $p^*(V_D-V_U)$ since the shape of the transition does not change. With W denoting the isothermal strain-energy per unit undeformed volume of a cylindrical section, the pressure work must equal W_D-W_U since the strain energy stored in the transition does not change under a steady-state advance of the front.

The deformation states in the transition are not purely cylindrical. Nevertheless, because the rubber is characterized by an energy function, W_D-W_U can be calculated using any deformation history which connects states U and D. Thus, if $p(V)$ denotes the relation depicted in Fig. 1 for purely cylindrical deformations, the strain energy difference equals the work in deforming the section from U to D through this deformation history. That is,

$$W_D - W_U = \int_{V_U}^{V_D} p(V)\,dV \tag{2.1}$$

The equation for p^* is therefore

$$p^*(V_D-V_U) = \int_{V_U}^{V_D} p(V)\,dV \tag{2.2}$$

with the well-known graphical solution requiring equality of the areas of the two lobes, $\mathscr{R}_1$ and $\mathscr{R}_2$, as indicated in Fig. 1.

The above derivation for steady-state propagation along the infinitely long balloon obviously applies whether or not the transition is advancing. The derivation can be reinterpreted as the invariance with respect to an arbitrary shift of the solution in the axial direction. In the terminology of phase transformations [3], (2.2) is the condition for the coexistence of two "phases", D and U, of the infinitely long balloon. The pressure p^* for coexistence is below the peak pressure needed to first form a bulge. For the rubber material analyzed in detail in [1], the initial bulging pressure is about twice p^*. This barrier to the formation of a transition is typical of each analog discussed here.

Yin [4] has given a rather complete and general analysis of the deformation of cylindrical membranes subject to internal pressure. We will draw from his work to show how (2.2) emerges from a direct integration of the equations governing axisymmetric deformations of a cylindrical membrane.

Consider a uniform long circular cylindrical membrane of an incompressible rubber-like material which is capped at its ends. The undeformed radius of the membrane is ρ. Attention is restricted to axisymmetric deformations due to internal pressure p. Let $w(\lambda_1,\lambda_2)$ denote the strain energy function of the rubber per unit undeformed area, where λ_1 and λ_2 are the meridional and azimuthal stretches. Based on earlier work of Pipkin [5], Yin has shown that the two equations of equilibrium can be reduced to the following two equations governing the deflection of the membrane:

$$\lambda_1 \frac{\partial w}{\partial \lambda_1} - w = \text{constant} \tag{2.3}$$

and

$$t_1 \cos \omega = \frac{1}{2}\lambda_2 \rho p \tag{2.4}$$

where $t_1 = \lambda_2^{-1}\partial w/\partial\lambda_1$ is the force per unit length of deformed membrane in the meridional direction and ω is the angle made by the meridional tangent with the axis of symmetry.

Using (2.4) to eliminate $\partial w/\partial\lambda_1$ in (2.3), one can readily show that (2.3) can be re-expressed as

$$pV\cos^{-2}\omega - W = \text{constant} \tag{2.5}$$

where, as before, W is the strain energy per unit undeformed volume of a meridional slice and V is the deformed volume of the same slice.

The constant can be evaluated using state U behind the transition for which $\omega = 0$, so that everywhere along the membrane

$$pV\cos^{-2}\omega - W = pV_U - W_U \tag{2.6}$$

In particular, on the other side of the transition in state D where ω again vanishes, (2.6) becomes

$$pV_D - W_D = pV_U - W_U \tag{2.7}$$

which is equivalent to (2.1) and (2.2).

3. NECK PROPAGATION ALONG CYLINDRICAL TENSILE SPECIMENS OF CERTAIN POLYMERIC MATERIALS

Figure 4, taken from the paper by G'Sell, Aly-Helal and Jonas [6], shows a sequence of pictures of the same tensile specimen taken over a progression of overall elongations. The specimen is a solid circular cylinder of high density polyethylene which has been tested in tension in a relatively stiff testing machine. The machine effectively imposes a constant rate of relative separation of the specimen ends. The load carried by the specimen is measured by a load cell (it is not prescribed). Although it may not be noticeable in the first picture of the sequence, a very slight reduction in cross-section has been introduced by machining at the central section of the specimen to induce the neck to set in near the center of the specimen.

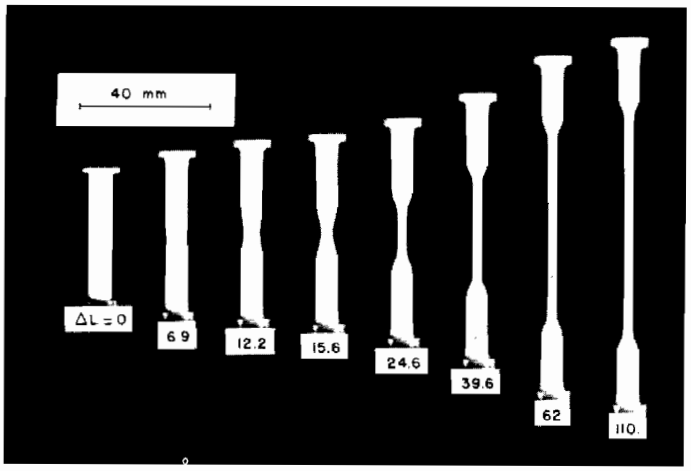

Fig. 4 A sequence of pictures of a solid cylindrical tensile specimen of high density polyethylene displaying neck propagation. (Figure taken from [6].)

The initial stages of neck formation shown in Fig. 4 are very similar to those observed in metal specimens. Significant necking becomes noticeable just following the peak in the overall load-elongation record, and the neck deepens and remains localized as the load continues to fall. In metals, this process continues with monotonically decreasing load until fracture processes interrupt the necking and the specimen fails. Certain polymer specimens, such as that in Fig. 4, propagate the neck once it has become fully localized. It is this aspect which we focus on here. G'Sell et al. [6] have published overall load-elongation records for their tests. These records are qualitatively similar to the overall pressure-volume curve for the cylindrical balloon previously discussed in Fig. 2. After a brief "transient" the neck transition attains a fixed shape and moves along the specimen at a constant velocity, assuming the overall elongation-rate is held constant. Under these steady-state propagation conditions the load is constant, and the radii of

the uniform sections of the specimen on either side of the transition do not change. The transition itself extends over an axial distance which is roughly equal to one diameter of the unnecked section.

Constitutive behavior of polymeric materials is not simple. Compared to metals, they have stronger thermal-mechanical coupling and a relatively stronger dependence on the rate of deformation. Moreover, like metals, their multi-axial stress-strain behavior is strongly path-dependent, even when rate-dependency is ignored. Nevertheless, it is very useful to consider a model rubber-like material (i.e., an incompressible, Green-elastic material) whose uniaxial stress-strain curve coincides with that displayed by the polymer at the representative rate of straining. The reason for this is that neck propagation is primarily a consequence of the qualitative shape of the uniaxial stress-strain curve of the material, as will be seen below. The analog between neck propagation in polymers and phase transitions was apparently noted as early as the late 1950's by Thompson and Tuckett (cf. discussion of the paper by Barenblatt [7]). Conditions for the coexistence of necked and unnecked states in a bar subject to uniaxial tension have been considered more recently by Ericksen [8] and James [3]. Here we will review the condition for steady-state propagation assuming the material is nonlinearly elastic and then discuss departures from such ideal behavior when the material is not elastic using results drawn from [2].

Consider a model incompressible, nonlinearly elastic material whose stress-strain behavior in uniaxial tension under isothermal conditions has the features shown in Fig. 5. Here two pairs of work conjugate variables have been used to display the tensile response. While the true stress-log strain curve may be monotonically increasing, the curve of nominal stress (force/original area) versus stretch is assumed to have a local maximum, a local minimum, and then increase monotonicaly to nominal stress levels well above

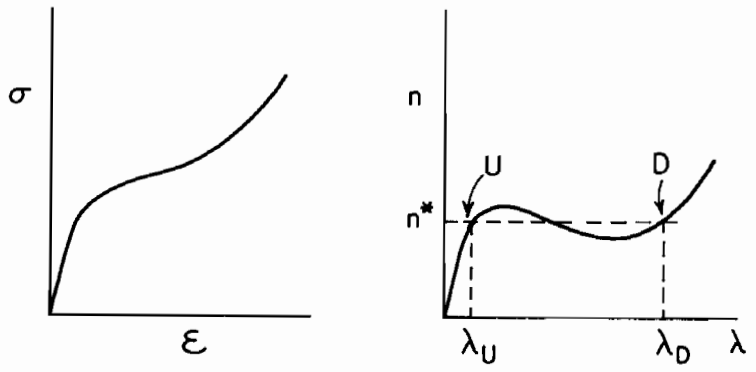

Fig. 5 Stress-strain data in uniaxial tension. True stress versus logarithmic strain on the left and nominal stress (load/original area) versus stretch on the right.

that at the local maximum. The idealized problem is considered for isothermal, steady-state neck propagation along an infinite uniform bar of this material. In the steady-state problem the transition between necked and unnecked regions translates with no shape change towards the unnecked region. An energy balance argument identical to that for the balloon leads to the equation

$$n^*(\lambda_D - \lambda_U) = W_D - W_U \qquad (3.1)$$

connecting the nominal stress for quasi-static propagation n^* (i.e., the load per original cross-sectional area) with the stretches in the necked (λ_D) and unnecked (λ_U) regions. Here W is the (isothermal) strain energy density of the material and W_D and W_U denote its values in the uniaxial states far ahead and far behind the transition.

The states of stress in the transition are not uniaxial. Nevertheless, the existence of the strain energy density function W permits us to evaluate $W_D - W_U$ using the uniaxial history $n(\lambda)$ to deform from state U to state D. Since the energy density difference is the work in deforming

from U to D , it follows that

$$W_D - W_U = \int_{\lambda_U}^{\lambda_D} n(\lambda)\,d\lambda \tag{3.2}$$

The graphical Maxwell-line solution based on (3.1) and (3.2) is indicated in Fig. 5. It has been tacitly assumed that the solution in the transition is smooth and consistent with quasi-static deformation. This places certain restrictions on W which have not been fully documented. Some polymeric materials whose true stress-strain data in tension has a sharp local maximum exhibit nonsmooth behavior in the form of shear bands, analogous to Lüders bands. But polymeric materials whose true stress-strain curve is monotonically increasing do not appear to give rise to any purely material instabilities, such as shear bands, in neck propagation and the neck transition is smooth.

Some sense of how accurately neck propagation in the nonlinearly elastic model material mimics necking of a more complicated polymeric material was obtained in [2]. In that paper the steady-state problem was formulated and solved approximately for an initially uniform, solid circular cylindrical bar. Two aspects of constitutive behavior departing from nonlinear elasticity were addressed: inherent path-dependence under multiaxial stressing histories, and rate-dependence. Each of these features invalidates the assumptions leading to (3.1) and (3.2) since the strain energy density function W no longer exists. Equation (3.1) continues to hold precisely if W_D-W_U is interpreted as the stress work experienced by a transverse slice of unit volume as it is engulfed by the transition and if n^* is the nominal axial stress averaged across the cross-section (i.e., load/original area, P/A_0). But this stress work difference can no longer be evaluated in terms of the uniaxial history. Now, even to determine quantities such as λ_D , λ_U and

P/A_0 associated with the steady-state solution far ahead and behind the transition, it is necessary to solve the entire problem, including the behavior in the transition.

In [2] the steady-state problem for a solid circular cylindrical bar was formulated as an axisymmetric 3-D flow problem in which the free-surface of the bar was determined as part of the solution process. Approximate solutions were generated using a variational principle together with a numerically implemented Galerkin-Ritz procedure. Here we will comment only on the results obtained for the history dependent constitutive model, the J_2 flow theory of plastic deformation (i.e., Prandtl-Reuss theory based on the Mises invariant). This is a rate-independent constitutive law which is fully specified after it has been made to coincide with data specifying material behavior in uniaxial tension. Calculations were performed for materials with specific uniaxial stress-strain curves chosen to approximate those measured for actual polymeric materials. The results were compared with the predictions based on (3.1) and (3.2) for the nonlinearly elastic model with precisely the same uniaxial stress-strain curve.

Characteristic of the plastic material is a considerably increased resistance to deformation in multiaxial deformation histories which are nonproportional, compared to the response of the corresponding nonlinearly elastic material. Since deformation histories of material elements passing through the neck are decidedly nonproportional, the plastic material offers more resistance to neck propagation than its nonlinearly elastic counterpart. For the examples investigated in [2] the nominal load associated with steady-state propagation was between 10 and 20 percent larger for the plastic bar than the elastic bar. The reduction in cross-section from U to D was generally somewhat greater for the plastic material. The work absorbed per slice of unit volume of material as it passes from far ahead to far behind the

transition, $W_D - W_U$, is about 30% greater for the plastic bar than the elastic bar. The solution indicates that the shape of the transition is not too different for the two bar materials. The transition is fairly sharp. Its axial extent is approximately one diameter of the unnecked bar.

4. BUCKLE PROPAGATION ALONG PIPES SUBJECT TO EXTERNAL PRESSURE

This phenomena is of some importance in the design of undersea pipelines against collapse [9, 10], and it is this application which provides the background for the work [1] summarized briefly below.

The buckling pressure of a long thin, circular cylindrical shell (pipe) subject to external pressure p is

$$p_c = \frac{E}{4(1-\nu^2)}\left(\frac{t}{R}\right)^3 \tag{4.1}$$

assuming the shell buckles in the linearly elastic range. Here E and ν are Young's modulus and Poisson's ratio of the material, which is assumed to be isotropic; t is the pipe thickness; and R is its radius. The buckling mode associated with (4.1) is a ring-like deformation in which each cross-section of the pipe undergoes the same ovalization, i.e., a plane strain ring deformation. An undersea pipeline usually has a ratio of t to R in the range 1/15 to 1/50 and is made of a steel with a yield stress which is sufficiently high such that a perfectly (or nearly perfect) circular pipe does undergo bifurcation from the circular state (i.e., does start to buckle) when the stresses are still in the elastic range. Thus, as long as the pipe is not unduly imperfect or damaged, (4.1) provides a good estimate of the maximum pressure the pipe can safely support.

If, however, the pipe suffers a substantial dent at some point along its length or if it buckles locally due to bending in the laying process, then a propagating buckle can be set into motion which spreads over the entire length of the pipe. A short section of a long pipe which has

experienced buckle propagation is shown in Fig. 6. The section was selected to show the plastically collapsed section and the transition to the unbuckled circular section. In a manner very similar to the two phenomena discussed earlier, the buckle propagation quickly settles down to a steady-state in which the transition remains fixed in shape and translates along the pipe at constant velocity, assuming the pressure is held constant [10]. The lowest pressure p^* at which steady-state propagation can occur is that associated with low-velocity, quasi-static propagation corresponding to negligible inertial effects. Moreover, the quasi-static propagation pressure p^* can be as little as .2 or even .1 of the "classical" buckling pressure p_c for typical pipe dimensions and materials. Thus a pipe which has suffered severe local damage is susceptible to collapse over its entire length at pressures well below what would normally be considered the buckling pressure.

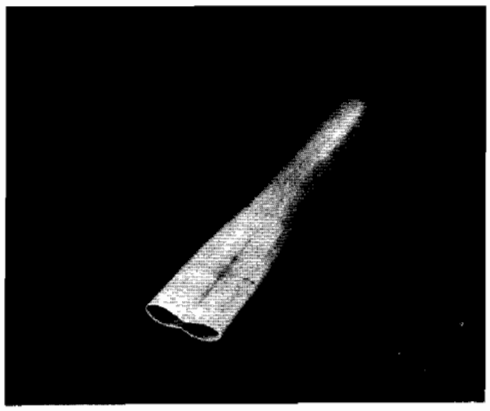

Fig. 6 Section of a pipe showing the transition between the buckled and unbuckled regions of the pipe (pipe section supplied by S. Kyriakides).

The approach put forward in [1] for predicting p^* made use of the buckling and post-buckling solution for a pipe undergoing plane strain ring deformations. The key

assumption, or approximation, in developing the model of the pipe is the representation of the pipe material by a nonlinearly elastic material (the deformation theory of plasticity) whose uniaxial stress-strain curve coincides with that of the actual material. This step, which ignores the path-dependence inherent to plastic flow, is analogous (but less drastic) to modeling a polymer by a nonlinearly elastic material, as discussed in the previous section. Invoking a nonlinearly elastic material permits us to connect the ring deformation states far ahead and far behind the transition using the same argument employed in the other two examples. In this way the extremely difficult problem governing behavior in the transition can be side-stepped.

A schematic plot of external pressure p as a function of cross-sectional area decrease ΔA is shown in Fig. 7 for an infinitely long circular cylindrical thin shell undergoing plane strain ring deformation. The yield stress of the material is such that bifurcation (the start of buckling) from the circular state occurs within the elastic range, as already discussed. As ovalization proceeds under slightly increasing pressure, plastic yielding (i.e., nonlinear elastic effects for the nonlinearly elastic material model) begins and a dramatic drop in pressure carrying capacity accompanies further ovalization. When the area decrease ΔA attains approximately 3/4 of the original cross-sectional area, opposite sides of the shell touch and provide an immediate bracing effect. Thereafter, the pressure rises steeply with relatively small additional area decrease.

The state U of the pipe well ahead of the transition is circular and well within the linear elastic range. The collapsed state D far behind the transition is a collapsed ring state. The energy balance argument for propagation of the buckle in the pipe of nonlinearly elastic material under quasi-static, steady-state conditions leads to

$$p^*(\Delta A_D - \Delta A_U) = \int_{\Delta A_U}^{\Delta A_D} p(\Delta A)\, d\Delta A \qquad (4.2)$$

Here $p(\Delta A)$ denotes relation between pressure and change of area for plane strain ring deformations so that the Maxwell-line construction for p^* applies, as indicated in Fig. 7.

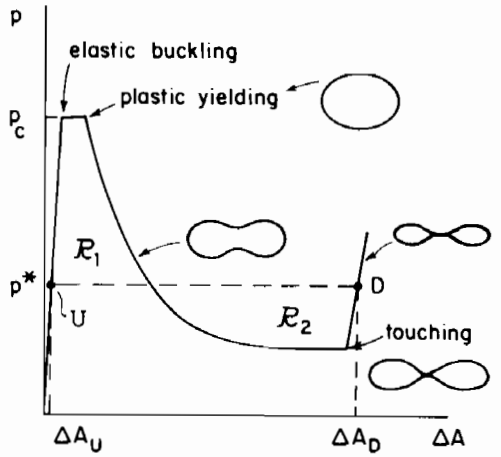

Fig. 7 Buckling and post-buckling of a ring of deformation theory material undergoing plane strain deformation. Schematic curve taken from [1].

Curves of $p(\Delta A)$ calculated using actual uniaxial stress-strain data are given in [1] along with the calculated values of p^*. Comparisons of the predicted values of p^* with experimentally measured quasi-static propagation pressures by Kyriakides are also given in [1] and generally excellent agreement was found. In every case, the theoretical estimate of p^* underestimated the actual propagation pressure, although in most instances only by a few percent. Qualitative arguments involving technical details of plasticity theory can be made to explain why the present simple theory should underestimate measured values of p^* and, additionally, why path-dependent flow effects in the transition area are not of major importance.

REFERENCES

1. Chater, E. and J. W. Hutchinson, On the propagation of bulges and buckles, J. Appl. Mech. (to appear - 1984).
2. Hutchinson, J. W. and K. W. Neale, Neck propagation, J. Mech. Phys. Solids 31 (1983), 405-426.
3. James, R. D., Co-existent phases in one-dimensional static theory of elastic bars, Arch. Rat. Mech. Anal. 72 (1979), 99-140.
4. Yin, W.-L., Non-uniform inflation of a cylindrical elastic membrane and direct determination of the strain energy function, J. Elasticity 7 (1977), 265-282.
5. Pipkin, A. C., Integration of an equation in membrane theory, Z. angen. Math. Phys. 19 (1968), 818.
6. G'Sell, C., N. A. Aly-Helal and J. J. Jonas, Effect of stress triaxiality on neck propagation during the tensile stretching of solid polymers, J. Mater. Sci. 18 (1983), 1731.
7. Barenblatt, G. I., Methods of combustion theory in the mechanics of deformation, flow, and fracture of polymers, in Deformation and Fracture of High Polymers (H. H. Rausch, J. A. Hassell and R. J. Jaffee, eds.), Plenum Press, 1974, 91-111.
8. Ericksen, J. L., Equilibrium of bars, J. Elasticity 5, (1975), 191-201.
9. Palmer, A. C. and J. H. Martin, Buckle propagation in submarine pipelines, Nature 254 (1975), 46-48.
10. Kyriakides, S. and C. D. Babcock, Experimental determination of the propagation pressure of circular pipes, ASME J. Pressure Vessel Tech. 103 (1981), 328-336.

The work of E.C. was supported in part by the Natural Sciences and Engineering Research Council of Canada and by the National Science Foundation under Grant MEA-82-13925. The work of J.W.H. was supported in part by the National Science Foundation under Grant MEA-82-13925 and by the Division of Applied Sciences, Harvard University. C. G'Sell supplied the photograph in Fig. 4.

Division of Applied Sciences
Harvard University
Cambridge, Massachusetts 02138